
Bounded-Distortion Metric Learning

Renjie Liao, Jianping Shi

The Chinese University of Hong Kong
rjliao, jpshi@cse.cuhk.edu.hk

Ziyang Ma

University of Chinese Academy of Sciences
maziyang08@gmail.com

Jun Zhu

Tsinghua University
dcszj@mail.tsinghua.edu.cn

Jiaya Jia

The Chinese University of Hong Kong
leojia@cse.cuhk.edu.hk

Abstract

Metric learning aims to embed one metric space into another to benefit tasks like classification and clustering. Although a greatly distorted metric space has a high degree of freedom to fit training data, it is prone to overfitting and numerical inaccuracy. This paper presents *bounded-distortion metric learning* (BDML), a new metric learning framework which amounts to finding an optimal Mahalanobis metric space with a bounded-distortion constraint. An efficient solver based on the multiplicative weights update method is proposed. Moreover, we generalize BDML to pseudo-metric learning and devise the semidefinite relaxation and a randomized algorithm to approximately solve it. We further provide theoretical analysis to show that distortion is a key ingredient for stability and generalization ability of our BDML algorithm. Extensive experiments on several benchmark datasets yield promising results.

1 Introduction

Distance metric learning is a fundamental problem in machine learning, since many learning algorithms, *e.g.*, k-nearest neighbors (kNN) and k-means, crucially rely on a “good” metric. The criteria of good metrics may differ in various learning tasks. For instance, in supervised learning, a common criterion is to learn a metric with a low empirical error [39], while in unsupervised learning, a good criterion is to learn a metric that minimizes the intra-cluster distance and simultaneously maximizes the inter-cluster distance [41].

In essence, metric learning aims to search a metric embedding to convert the original metric space (*e.g.*, Euclidean) into a new one, which better suits learning tasks with regard to the above criteria. Such an embedding intrinsically induces distortion - a concept in the theory of metric embedding [4], which intuitively measures the effort to reshape the metric space.

Although a large-distorted metric space can have a high degree of freedom to describe data, it may be prone to overfitting. In fact, we will theoretically validate the intuition later by proving that in our case of Mahalanobis metric learning, the generalization bound depends increasingly on the distortion. Moreover, the numerical inaccuracy would also be a problem if the distortion is extremely large. We will show that the distortion of Mahalanobis metric learning is the condition number of the parameter matrix. Inevitably, a large distortion would make the matrix ill-conditioned.

In order to balance the fitness of the learned the metric space to training data and the distortion of the underlying metric embedding, we present *bounded-distortion metric learning* (BDML), a generic framework that imposes a bounded-distortion constraint to the learning objective. While it fits various metric learning objectives, we concentrate on learning Mahalanobis metric space, which leads to a semidefinite programming (SDP) formulation.

We approach the SDP via a bisection method, which involves solving a sequence of convex feasibility problems with fast multiplicative weights update [23]. Moreover, to deal with the pseudo-metric learning, we apply the spectral decomposition to the parameter matrix and perform joint learning of dimension reduction mapping and metric. We relax the resultant non-convex quadratic constrained quadratic programming (QCQP) to a SDP and achieve the approximation by a randomized algorithm. Theoretical analysis is provided to reveal that distortion has a direct impact on the stability and generalization ability of a class of metric learning algorithms. Experimental results on several benchmark datasets manifest the usefulness of our BDML.

2 Related Work

Metric learning algorithms can be categorized according to different criteria, such as Mahalanobis [41, 37, 3] and non-Mahalanobis [24, 32, 14] methods; probabilistic [20, 8] and non-probabilistic [21, 38] methods; unsupervised [34], supervised [42] and semi-supervised [41] methods; and global [9] and local [13] methods.

Based on the type of constraints, we can also classify them into pairwise and triplet-wise ones. Pairwise methods [41, 7] often add constraints to enforce distances between pairs of dissimilar points are larger than a given threshold. Representative methods in the triplet group are the large-margin nearest neighbor [39] and its variants [24]. They exploit the local triplet constraints to assure that the distance between any point and its different-class neighbour should be at least one unit margin further than the distance between it and its same-class neighbour. Intuitively, if these triplet constraints are well satisfied, the empirical loss of kNN would be small.

Metric learning is closely related to *metric embedding*, an important topic in theoretical computer science that has played an important role to design approximation algorithms. One line of research focuses on how to embed a finite metric space into normed spaces with a low distortion [4, 19], *i.e.*, preserving the structure of the original metric space. Metric learning is also related to manifold learning [14] and kernel learning [26]. Learning a distance metric function amounts to learning a kernel function that measures the similarity between points.

3 Bounded-Distortion Metric Learning

Before going to details, we introduce necessary notations. $\mathbb{S}^d = \{M | M \in \mathbb{R}^{d \times d}, M^\top = M\}$ is the space of all $d \times d$ real symmetric matrices equipped with the Frobenius inner product $A \bullet B = \text{Tr}(A^\top B)$. The positive semidefinite (PSD) cone and positive definite (PD) cone are denoted as $\mathbb{S}_+^d = \{M | M \in \mathbb{S}^d, M \succeq 0\}$ and $\mathbb{S}_{++}^d = \{M | M \in \mathbb{S}^d, M \succ 0\}$ respectively. The convex set $\mathbb{P}_R^d = \{M | M \in \mathbb{S}_{++}^d, \text{Tr}(M) \leq R\}$ is also used. The trace bound R in \mathbb{P}_R^d is a parameter to ensure a bounded domain for M . \mathbb{R}_+^d denotes the d -dimensional nonnegative orthant.

3.1 Distortion of Metric Embedding

A definition of metric space is the following.

Definition 1. A pair $(\mathcal{X}, d_{\mathcal{X}})$ is called a metric space, where \mathcal{X} is a set of points and $d_{\mathcal{X}} : \mathcal{X} \times \mathcal{X} \rightarrow [0, \infty)$ is a distance function satisfying the following conditions for all $x_i, x_j, x_k \in \mathcal{X}$:

- $d_{\mathcal{X}}(x_i, x_j) = 0$, iff $x_i = x_j$,
- $d_{\mathcal{X}}(x_i, x_j) = d_{\mathcal{X}}(x_j, x_i)$,
- $d_{\mathcal{X}}(x_i, x_j) + d_{\mathcal{X}}(x_j, x_k) \geq d_{\mathcal{X}}(x_i, x_k)$.

A Mahalanobis metric space is a metric space equipped with a Mahalanobis distance function, which often takes the form of $d_{\mathcal{X}}(x_i, x_j) = \sqrt{(x_i - x_j)^\top M (x_i - x_j)}$, parameterized by a PD matrix M , *i.e.*, $M \in \mathbb{S}_{++}^d$. In the metric learning literatures, a PSD M is usually adopted, thus the induced distance function is a pseudo-metric in the strict sense. We now focus on the PD case and defer the PSD one to Sect. 5. Obviously, the Euclidean space is a special Mahalanobis metric space where M is an identity matrix. Note that we deal with the squared Mahalanobis distance since it does not affect learning methods (*e.g.*, kNN) that are based on relative distances.

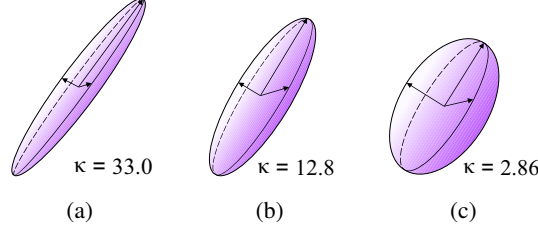


Figure 1: Ellipsoids with various condition numbers, where (a) and (c) have the same logDet value ≈ 3.5 ; (b) and (c) have the same F-norm value ≈ 7.2 .

We can embed one metric space into another with a certain degree of distortion. The formal definition of metric embedding and its distortion are as follows [4, 19],

Definition 2. Let $(\mathcal{X}, d_{\mathcal{X}})$ and $(\mathcal{Y}, d_{\mathcal{Y}})$ be two metric spaces. A mapping $f : \mathcal{X} \rightarrow \mathcal{Y}$ is said to be a c -embedding if there exists $r > 0$ such that for all $x, y \in \mathcal{X}$,

$$r \cdot d_{\mathcal{X}}(x, y) \leq d_{\mathcal{Y}}(f(x), f(y)) \leq cr \cdot d_{\mathcal{X}}(x, y). \quad (1)$$

The distortion of f is defined as the infimum of all c such that f is a c -embedding.

Distortion is a measure of the distance between two metric spaces and plays an important role in the theory of metric embeddings. Later we will show that distortion is essential to stabilize a class of metric learning algorithms.

In Mahalanobis metric learning, given an Euclidean metric space (\mathcal{X}, d_I) , we learn a metric embedding $f_{I \rightarrow M}$, which returns us a desired Mahalanobis metric space (\mathcal{X}, d_M) . We have the following proposition to specify the distortion of this metric embedding.

Proposition 1. *The distortion of the metric embedding $f_{I \rightarrow M}$ is the condition number $\kappa(M)$.*

Due to the page limit, we focus on presenting important results in this paper and defer all proofs to the appendix in the supplementary file.

3.2 Geometric Meaning of Distortion

Distortion can be intuitively regarded as a complexity measure of metric embedding. From a geometric perspective, it possesses an intrinsically different meaning compared to other complexity measures in previous work, including the log determinant (logDet) [7] and Frobenius norm (F-norm) [21]. Specifically, we focus on analyzing the metric embedding $f_{I \rightarrow M}$ and consider an origin-centered ellipsoid $\mathcal{E} = \{x \in \mathbb{R}^d | x^\top M x \leq 1\}$ for simplicity.

Let $\{\lambda_i\}_{i=1}^d$ be the set of eigenvalues of M . It is well-known that the logarithmic volume of \mathcal{E} is $\log(V(\mathcal{E})) = \log(\gamma) - \frac{1}{2} \log \text{Det}(M)$, where γ is the volume of the unit sphere in \mathbb{R}^d . The squared F-norm of M is defined as $\|M\|_F^2 = \sum_{i=1}^d 1/r_i^4$, where $r_i = 1/\sqrt{\lambda_i}$ is the length of the i -th semi-axis. The condition number is $\kappa(M) = r_{\max}^2/r_{\min}^2$. In other words, logDet measures the volume variation; F-norm indicates the change of overall lengths of semi-axes; while the condition number describes the length ratio variation between the longest and the shortest semi-axis. As illustrated in Fig. 1, it is possible that a metric with a small logDet or F-norm value is ill-conditioned, *i.e.*, the ellipsoid is extremely elongated. Therefore, rather than focusing on the absolute variation, distortion measures the relative one, thus enabling higher freedom and directly controlling the well-conditioning property.

3.3 Pair and Triplet Constrained BDML

Given a training dataset $D = \{(x_i, y_i)\}_{i=1}^N$, where $x_i \in \mathbb{R}^d$ is a data point and y_i is the corresponding class label, our task is to obtain a Mahalanobis distance metric space (\mathcal{X}, d_M) , where d_M is the distance function defined as, $d_M(x_i, x_j) = (x_i - x_j)^\top M (x_i - x_j) = M \bullet X_{ij}$, and $M \in \mathbb{S}_{++}^d$. Here we define $X_{ij} = (x_i - x_j)(x_i - x_j)^\top$ for notation simplicity.

Algorithm 1 : A Bisection Method

- 1: Given the interval of g^* as $[L, U]$, tolerance $\epsilon > 0$,
 - 2: **Repeat**
 - 3: $\bar{g} = (L + U)/2$.
 - 4: Solve the convex feasibility problem (4).
 - 5: **If** problem (4) is feasible: $U = \bar{g}$.
 - 6: **Else:** $L = \bar{g}$.
 - 7: **Until** $U - L \leq \epsilon$
 - 8: Return the final objective value as \bar{g} .
-

We now present two notable formulations of our bounded-distortion metric learning (BDML), which correspond to two types of constraints in the literature of metric learning, *i.e.*, pairwise ones and triplet-wise ones. Specifically, for any data point x_i , we consider its k -nearest neighbours set Ω_i . Following [39], two types of neighbor points are distinguished. They are *target neighbors* that share the same class label with x_i , and *imposter neighbors* that have different class labels with x_i .

Let $\mathcal{S} = \{(i, j) | x_j \in \Omega_i, y_j = y_i\}$ and $\mathcal{I} = \{(i, j) | x_j \in \Omega_i, y_j \neq y_i\}$ be the sets of all index pairs of target neighbors and imposter neighbors respectively. $\mathcal{T} = \{(i, j, k) | (i, j) \in \mathcal{S}, (i, k) \in \mathcal{I}\}$ denotes the set of all such index triplets.

We define the pair-constrained bounded-distortion metric learning (p -BDML) as

$$\begin{aligned} \min_{M \in \mathbb{P}_R^d} \quad & \frac{1}{n} \sum_{(i,j) \in \mathcal{S}} M \bullet X_{ij} \\ \text{s.t.} \quad & M \bullet X_{ij} \geq \mu, \quad \forall (i, j) \in \mathcal{I}, \\ & \kappa(M) \leq K, \end{aligned} \tag{2}$$

where $n = |\mathcal{S}|$ and K is a parameter to control the upper bound of distortion. Pair-wise constraints are designed to pull two imposter neighbors farther than a margin or push two target neighbors closer than a margin in literatures. Here we only consider the former purpose and minimize the average distance of target neighbors as in [41].

The triplet-constrained bounded-distortion metric learning (t -BDML) is formulated as,

$$\begin{aligned} \min_{M \in \mathbb{P}_R^d} \quad & \frac{1}{n} \sum_{(i,j) \in \mathcal{S}} M \bullet X_{ij} \\ \text{s.t.} \quad & M \bullet X_{ik} - M \bullet X_{ij} \geq \mu, \quad \forall (i, j, k) \in \mathcal{T}, \\ & \kappa(M) \leq K. \end{aligned} \tag{3}$$

The above inequality constraint of triplet nearest neighbors ensure that any given point has its imposter neighbors at least one unit margin farther than its target neighbors. Note that the unit margin in [39] can be set as a arbitrarily positive constant, since it only affects the scale of M . In our case, since we consider a bounded domain of M (*i.e.*, $M \in \mathbb{P}_R^d$), the margin μ is treated as a positive parameter.

Note that the bounded-distortion constraint $\kappa(M) \leq K$ implies that M should be PD since otherwise $\kappa(M)$ is unbounded. Albeit nonconvex, the condition number function is quasi-convex. It means all its sublevel sets are convex. This property enables us to transform p -BDML and t -BDML to the standard formulation of SDP.

4 A Bisection Algorithm with Multiplicative Weights Update

We now present a bisection algorithm for approaching our p -BDML and t -BDML, which essentially solves a sequence of convex feasibility problems. For each feasibility problem, we resort to the multiplicative weights update (MWU) method [23, 1], which is a meta algorithm and has many variants in different disciplines. The reason of choosing MWU is that it generates an approximate solution with guaranteed constraint violation – it is important for the analysis in Sec. 6 to hold.

4.1 Sequential Convex Feasibility Problems

In what follows, we only describe the convex feasibility problem for p -BDML, since the formulation for t -BDML only differs in constraints. We denote the objective function as $g(M) = G \bullet M$ where $G = \frac{1}{n} \sum_{(i,j) \in \mathcal{S}} X_{ij}$. Its optimal value g^* is assumed to lie in the initial interval $[L, U]$, where L and U are set as 0 and $g(I)$ respectively. I is the identity matrix. Our bisection algorithm estimates g and narrows down the interval by half in each iteration. The procedure of the bisection algorithm is outlined in Alg. 1.

Specifically, if g is not larger than \hat{g} in one iteration, we solve a convex feasibility problem as

$$\begin{aligned} \text{find} \quad & M \in \mathbb{P}_R^d, \quad \alpha > 0 \\ \text{s.t.} \quad & G \bullet M \leq \bar{g}, \\ & M \bullet X_{ij} \geq \mu, \quad \forall (i, j) \in \mathcal{I}, \\ & \alpha I \preceq M \preceq \alpha K I. \end{aligned} \tag{4}$$

Here we introduce a positive auxiliary variable α and transform the bounded-distortion constraint into two generalized inequality constraints. The resultant convex feasibility problem can be approximately solved by the efficient MWU method, to be elaborated on in the next section.

4.2 Multiplicative Weights Update Method

Before applying MWU method, we reformulate the feasibility problem (4) to a general form via introducing slack variables $M_1 = M - \alpha I$ and $M_2 = \alpha K I - M$. Then we construct a sparse symmetric matrix $Y \in \mathbb{P}_R^{3d+1}$ of which the block diagonal entries are M , M_1 , M_2 and α . All constraints except \mathbb{P}_R^{3d+1} in (4) are rewritten as $J_i \bullet Y \geq h_i$. \mathbb{P}_R^{3d+1} can be deemed as an easy constraint, contrary to each hard constraint $J_i \bullet Y \geq h_i$. With this change, we obtain the equivalent formulation of (4) as

$$\begin{aligned} \text{find} \quad & Y \in \mathbb{P}_R^{3d+1} \\ \text{s.t.} \quad & J_i \bullet Y \geq h_i, \quad \forall i = 1, \dots, m. \end{aligned} \tag{5}$$

The number of constraints is $m = |\mathcal{I}| + 4d^2 + 2$. We also introduce a closely related feasibility problem as

$$\begin{aligned} \text{find} \quad & Y \in \mathbb{P}_R^{3d+1} \\ \text{s.t.} \quad & \sum_{i=1}^m p_i (J_i \bullet Y - h_i) \geq 0. \end{aligned} \tag{6}$$

Here $\mathbf{p} = [p_1, \dots, p_m]^\top$ is a probability vector, i.e., $\forall i, p_i \geq 0$ and $\sum_{i=1}^m p_i = 1$. Note that this problem only contains 2 constraints, easy to solve. The relationship between problem (5) and (6) is summarized by the following lemma.

Lemma 1. *If problem (5) has a feasible solution Y^* , given any probability \mathbf{p} , then Y^* is feasible for problem (6). Equivalently, if there exists a probability \mathbf{p} such that problem (6) is infeasible, then problem (5) is infeasible.*

With the lemma, we now describe the MWU method for approaching problem (5). Basically, MWU maintains a weight vector $\mathbf{w} \in \mathbb{R}_+^m$, where each entry w_i represents the importance of the i -th constraint. It iteratively solves problem (6) and updates weights \mathbf{w} according to the constraint satisfaction $J_i \bullet Y - h_i$. Intuitively, if one constraint is more satisfied, the corresponding importance should be less and we should decrease its weight.

In t -th round of the algorithm, we get a probability vector $\mathbf{p}^{(t)}$ by normalizing the nonnegative weights $\mathbf{w}^{(t)}$. Then we solve the 2-constraint feasibility problem (6) by maximizing $\sum_{i=1}^m p_i (J_i \bullet Y^{(t)} - h_i)$ over \mathbb{P}_R^{3d+1} . If the maximum value is greater than 0, we take the corresponding $Y^{(t)}$ as a feasible solution. Otherwise (6) is infeasible. We call the solver of problem (6) as an ORACLE.

Implementing ORACLE needs to compute the largest eigenvector of the matrix $C = \sum_{i=1}^m p_i [J_i - (h_i/R)I]$, which can be efficiently handled by Lanczos algorithm. Here R is the trace bound parameter in \mathbb{P}_R^{3d+1} .

Algorithm 2 : Multiplicative Weights Update Method

```
1: Initialization: Fix a  $\varepsilon \leq 1/2$ , for each constraint, associate the weight  $w_i^{(1)} = 1$ .
2: For  $t = 1, 2, \dots, T$ :
3:   Normalize  $\mathbf{w}^{(t)}$  to get the probability vector  $\mathbf{p}^{(t)}$ .
4:   Call the ORACLE with  $\mathbf{p}^{(t)}$ .
5:   If ORACLE succeeds to find a solution  $Y^{(t)}$ 
6:      $\eta_i^{(t)} = \frac{1}{\rho}[J_i \bullet Y^{(t)} - h_i]$ .
7:      $w_i^{(t+1)} = w_i^{(t)}(1 - \varepsilon\eta_i^{(t)})$ .
8:   Else
9:     Return that the problem is infeasible.
10:  End
11: End
12: Return  $\bar{Y} = (\sum_{t=1}^T Y^{(t)})/T$  as a final solution.
```

Assuming ORACLE obtains a feasible solution $Y^{(t)}$, we denote the normalized satisfaction of i -th constraint of problem (5) as $\eta_i^{(t)} = \frac{1}{\rho}[J_i \bullet Y^{(t)} - h_i]$. Here ρ is called the *width* parameter, satisfying that $\forall i, |J_i \bullet Y^{(t)} - h_i| \leq \rho$. We update the weights as $w_i^{(t+1)} = w_i^{(t)}(1 - \varepsilon\eta_i^{(t)})$, where ε is a parameter smaller than $1/2$. Hence, $w_i^{(t+1)}$ is smaller than $w_i^{(t)}$ if $\eta_i^{(t)} > 0$, and its value increases otherwise.

The algorithm is depicted in Alg. 2. After T rounds, the averaged solution $\bar{Y} = (\sum_{t=1}^T Y^{(t)})/T$ is returned. We have the Theorem 1 following [1] to guarantee that either \bar{Y} achieves a predefined accuracy or we claim that the original problem (5) is infeasible.

Theorem 1. Let $\delta > 0$ be a given additive error¹. Alg. 2 either solves problem (5) up to δ , or correctly concludes that it is infeasible, making $O(\frac{\rho^2 \ln(m)}{\delta^2})$ calls to the ORACLE.

5 Pseudo-Metric & Dimension Reduction

In this section, we deal with the case of pseudo-metric, *i.e.*, M is PSD. In the literature of Mahalanobis metric learning, a PSD M is beneficial due to the existence of decomposition $M = C^\top C$, where $C \in \mathbb{R}^{q \times d}$. The distance function could be rewritten as $d(x, y) = \|Cx - Cy\|^2$. It thus removes the PSD constraint and allows flexible dimension reduction by choosing $q < d$.

In our setting, a PSD M could be problematic if it has an unbounded condition number. According to the spectral theorem, decomposition $M = Q^\top \Lambda Q$ is applicable, where $\Lambda \in \mathbb{R}^{q \times q}$ is a diagonal matrix with eigenvalues of M , $Q \in \mathbb{R}^{q \times d}$ has orthonormal rows and q is the rank of M . We can also choose different q to form different low rank approximation of M . Hence Q and Λ act as a dimension-reduction mapping and a dimension-wise scaling operation respectively.

By replacing M with the decomposition and adding orthogonal constraints for Q in original BDML, we can conduct the pseudo-metric learning via alternatively optimizing Q and Λ . Specifically, when Q is fixed, optimizing the diagonal Λ is just a simple case of original BDML. Nevertheless, optimizing Q with a known Λ is not straightforward. Especially, in the case of p -BDML, when Λ is fixed such that $\Lambda \in \mathcal{P}$ and $\kappa(\Lambda) \leq K$, the problem (2) can be reformulated as below,

$$\begin{aligned} \min_{Q \in \mathbb{R}^{q \times d}} \quad & \frac{1}{n} \sum_{(i,j) \in \mathcal{S}} X_{ij} \bullet (Q^\top \Lambda Q) \\ \text{s.t.} \quad & X_{ij} \bullet (Q^\top \Lambda Q) \geq \mu, \quad \forall (i, j) \in \mathcal{I}, \\ & QQ^\top = I. \end{aligned} \tag{7}$$

Note this learning problem is nontrivial due to the fact that optimizing Q is a quadratic constrained quadratic programming (QCQP). To overcome the difficulty, we have the following proposition,

¹Additive error up to δ means that, any constraint is violated at most δ , *i.e.*, $\forall i, J_i \bullet Y - h_i \geq -\delta$.

Algorithm 3 : Gaussian Randomization Procedure

- 1: **Initialization:** Given the optimal solution \tilde{Q}^* , iteration number T' , ratio γ and tolerance ϵ .
 - 2: **For** $t = 1, 2, \dots, T'$:
 - 3: Sample $\xi_t \sim \mathcal{N}(0, \tilde{Q}^*)$.
 - 4: **End**
 - 5: $\xi = \arg \min_{\xi_t} \frac{1}{n} \sum_{(i,j) \in \mathcal{S}} \xi_t^\top \tilde{X}_{ij} \xi_t$.
 - 6: Reshape ξ from $\mathbb{R}^{qd \times 1}$ to $\mathbb{R}^{q \times d}$.
 - 7: Return ξ as the approximate solution of problem (7).
-

Proposition 2. Problem (7) can be relaxed to a SDP as following,

$$\begin{aligned}
 \min_{\tilde{Q} \in \mathbb{S}_+^{qd}} \quad & \frac{1}{n} \sum_{(i,j) \in \mathcal{S}} \tilde{X}_{ij} \bullet \tilde{Q} \\
 \text{s.t.} \quad & \tilde{X}_{ij} \bullet \tilde{Q} \geq \mu, & \forall (i,j) \in \mathcal{I}, \\
 & A_{uv} \bullet \tilde{Q} = b_{uv}, & \forall (u,v) \in \mathcal{C},
 \end{aligned} \tag{8}$$

where $\tilde{X}_{ij} = X_{ij} \otimes \Lambda$ and \otimes stands for Kronecker product. A_{uv} is a block diagonal matrix which contains d identical blocks $B_{uv} \in \mathbb{R}^{q \times q}$. (u, v) and (v, u) -th entries of B_{uv} are 1 while others are 0. $b_{uv} = 2$ if $u = v$, otherwise $b_{uv} = 0$. $\mathcal{C} = \{(u, v) \in [q] \times [q] | u \leq v\}$ and $[q] = \{1, \dots, q\}$.

This proposition shows that when Λ is fixed we can learn Q by solving the above SDP relaxation. Moreover, since the equality constraints in (8) imply $\text{Tr}(\tilde{Q}) = q$, we thus can exploit the MWU method again.

Denoting the optimal objective values of problem (7) and (8) as ϱ_{qp} and ϱ_{sdp} respectively, it is obvious that $\varrho_{sdp} \leq \varrho_{qp}$. Hence we aim at up-bounding ϱ_{qp} . Specifically, once we obtained the optimal solution \tilde{Q}^* of problem (8), we construct an approximate solution ξ problem (7) based on a Gaussian randomization procedure shown in Alg. 3. We prove the following theorem to assure that in the worst case Alg. 3 would possibly generate an approximate solution with approximation ratio ω .

Theorem 2. If the optimal solution of problem (8) is \tilde{Q}^* and $\xi \in \mathbb{R}^{qd}$ is a random vector generated from the real-valued normal distribution $\mathcal{N}(0, \tilde{Q}^*)$, then for any $\gamma > 0$, $\epsilon \geq 0$ and $\omega \geq 1$, we have,

$$\begin{aligned}
 \text{Prob} \left(\nu \geq \gamma \mu \ \& \ \zeta \leq \epsilon \ \& \ \xi^\top \tilde{G} \xi \leq \omega \tilde{G} \bullet \tilde{Q}^* \right) \geq 1 - |\mathcal{I}| \max \left(\sqrt{\gamma}, \frac{2(r-1)\gamma}{\pi-2} \right) \\
 - r \exp \left(-\frac{1}{2} (\omega - \sqrt{2\omega-1}) \right) - \frac{rq(q+1)}{2} \left[\exp \left(-\frac{(\tau-1)^2}{4} \right) + \exp \left(-\frac{\epsilon^2}{8rdq^2} \right) \right],
 \end{aligned}$$

where $r = \text{rank}(\tilde{Q}^*)$ and $\tau = \sqrt{\frac{\epsilon}{q} \left(\frac{2}{rd} \right)^{1/2} + 1}$. ν , ζ and \tilde{G} are defined respectively as $\nu = \min_{(i,j) \in \mathcal{I}} \xi^\top \tilde{X}_{ij} \xi$, $\zeta = \max_{(u,v) \in \mathcal{C}} |\xi^\top A_{uv} \xi - b_{uv}|$ and $\tilde{G} = \frac{1}{n} \sum_{(i,j) \in \mathcal{S}} \tilde{X}_{ij}$.

Remark. This theorem indicates that with well chosen γ and ϵ , Alg. 3 can generate an approximate solution for (7) with guaranteed approximation ratio even in the worst case. For example, we can consider a real case with $q = 10$, $d = 100$ and the number of constraints $|\mathcal{I}| = 100$. By choosing $\gamma = \pi/16|\mathcal{I}|^2$, $\epsilon = 40q\sqrt{rd}$ and with appropriate rank reduction on \tilde{Q}^* as [30], it can be shown that after running Alg. 3 for 100 iteration, we have very high probability² such that $\frac{1}{\omega} \varrho_{qp} \leq \varrho_{sdp} \leq \varrho_{qp}$, where $\omega = 10$. However, the price we pay is that the orthogonal constraints are loosely satisfied. In practice, we found that the resultant approximate solution works well, which indicates that removing orthogonal constraints and transforming Λ to a full rank matrix may also be an alternative modeling choice.

As for the pseudo-metric learning of t -BDML, we can still use the above algorithm to obtain an approximate solution. However, Theorem 2 does not stand in this case since not all \tilde{X}_{ij} of t -BDML are PSD.

²The probability is at least 0.999828.

6 Generalization Bound for BDML

To theoretically investigate whether the distortion has an impact on the generalization ability, we derive the generalization bound of our BDML following the stability analysis of learning algorithms [5, 36].

Before diving into the details, we first introduce one assumption that we only consider the case where the metric matrix is full rank. Then we clarify some preliminary notations. Each training sample z inside the training set D is drawn i.i.d. from some unknown distribution \mathcal{D} . And the range of z is denoted as \mathcal{Z} . D^i is a perturbed set of D obtained via replacing i -th sample with a new sample drawn from \mathcal{D} , i.e., $D^i = \{D \setminus z_i \cup z'_i\}$, where $z'_i \sim \mathcal{D}$. We make a mild assumption that all data points are contained in a Γ -ball, i.e., $\|x\|_2 \leq \Gamma$. We denote the learning algorithm as \mathcal{A} , the *true risk* or *generalization error* as $\mathcal{R}(\mathcal{A}, D)$ and the *empirical risk* as $\mathcal{R}_{emp}(\mathcal{A}, D) = \frac{1}{n} \sum_k \ell(\mathcal{A}, z_k)$, where in our case the loss function $\ell = M \bullet X_{ij}$ and $n = |S|$. Based on [5], we define the Uniform-Replace-One stability as,

Definition 3. An algorithm \mathcal{A} has Uniform-Replace-One stability β with respect to the loss function ℓ if $\forall D \in \mathcal{Z}^n, \forall i \in \{1, \dots, n\}$,

$$\|\ell(\mathcal{A}_D, \cdot) - \ell(\mathcal{A}_{D^i}, \cdot)\|_\infty \leq \beta. \quad (9)$$

Here \mathcal{A}_D means the learning algorithm \mathcal{A} is trained on the dataset D . Note that our definition is stronger than the one proposed in [36], thus being more restrictive. We have the following lemma, which specifies the uniform-RO stability of our BDML.

Lemma 2. The Uniform-Replace-One stability of our BDML algorithm with respect to the given loss function ℓ is $\beta = \frac{4(K+1)R\Gamma^2}{d}$.

This lemma indicates that the Uniform-Replace-One stability of \mathcal{A} is positively correlated with the bound of distortion K . It means a low distortion of metric embedding would lead to a stable algorithm. Although β does not depend decreasingly on the number of samples n , which may not be seen as *stable* in some sense [5], it is clear that the stability can be controlled by the distortion. With this stability result, we further prove the following generalization bound, which theoretically explains the relationship between distortion and generalization error.

Theorem 3. For any metric learning algorithm \mathcal{A} with Uniform-Replace-One stability β with respect to the given loss function ℓ , we have with probability at least $1 - \delta$,

$$\mathcal{R}(\mathcal{A}, D) \leq \mathcal{R}_{emp}(\mathcal{A}, D) + 2\Gamma \sqrt{\frac{KR}{d\delta} \left(\frac{2KR\Gamma^2}{nd} + 3\beta \right)}.$$

Specifically, for our BDML algorithm,

$$\mathcal{R}(\mathcal{A}, D) \leq \mathcal{R}_{emp}(\mathcal{A}, D) + \frac{2R\Gamma^2}{d} \sqrt{\frac{2K}{\delta} \left(\frac{K}{n} + 6K + 6 \right)}.$$

Remark. There are several interesting things to note regarding to this theorem.

First, it explains our intuitive conjecture that a large distortion would incur overfitting during metric learning. It encourages us to choose a small value of K to improve the generalization ability of \mathcal{A} . On the other side, setting K as small as possible is unwise, since it would constrain our hypothesis class too much and thus may increase both the *true risk* and *empirical risk*. Therefore, it suggests choosing moderately small values of K in practice via cross validation.

Second, the generalization error tends to decrease with the increase of the dimension d . This phenomenon seems to be a bit counter-intuitive since it implies that our method becomes more stable in higher dimensional feature space. However, this does happen only if the previous assumption holds, i.e., M is full rank. In this case, the increase of the dimension squash the range of the spectrum of M since the trace bound R and distortion bound K are fixed. If M is instead rank-deficient, the above analysis does not stand. In particular, the bound will have a dependency on the rank of M and its perturbation. This means that naively increasing the feature dimension by adding zero will not make the bound tighter. We will illustrate this issue in the appendix.

Dataset	Wine	Iris	Diabetes	Waveform	Segment
Euc	3.46(3.60)	5.11(2.58)	31.09(2.03)	18.87(0.65)	5.61(0.92)
Xing	4.04(4.00)	6.67(3.11)	32.09(3.56)	16.43(1.00)	5.26(0.60)
LMNN	3.08(2.07)	4.22(1.95)	29.70(3.20)	18.61(0.72)	3.69(0.70)
ITML	1.15 (2.07)	4.44(2.57)	29.96(2.97)	15.94(0.83)	5.02(0.70)
BoostMetric	2.31(2.18)	3.56(2.52)	26.78(2.12)	16.86(0.90)	4.21(0.48)
p -BDML	2.83(1.3)	3.11(2.61)	27.57(2.21)	15.78(0.60)	4.21(0.79)
t -BDML	2.26(2.30)	2.44 (1.64)	26.43 (2.30)	15.34 (0.72)	3.62 (0.34)

Table 1: Comparison of average test errors (%) and standard deviations on UCI datasets.

7 Experiments

We present empirical evaluations of our BDML algorithm on a wide range of tasks, including classification on several UCI datasets [2], domain adaptation on medium-scale datasets [35], and face verification on the large-scale LFW dataset [18]. Before presenting the results, we first discuss a practical strategy to speed up the bisection method, since it is sometimes hard to estimate a tight interval of the optimal objective value in advance. Specifically, we select several fixed upper bounds and then solve the convex feasibility problem (4) in parallel. If the trial is successful, we use it to shrink the upper bound, otherwise we shrink the lower bound. This procedure provides us a largely reduced interval with time cost as small as one call of MWU solver. Note that we set parameters via cross validation. The impact of different parameters and runtime are provided in the appendix due to space limits.

7.1 Classification

We first conduct classification experiments on several UCI datasets, including Wine, Iris, Diabetes, Segment and Waveform, to validate the effectiveness of our BDML. We randomly split datasets into 70% for training and 30% for testing and report the average test errors and standard deviations by repeating the random splits for 10 times. We compare with the baseline of Euclidean metric and several strong competitors like Xing [41], LMNN [39], ITML [7] and BoostMetric [38]. The neighborhood size of kNN classifier is 3 and all metric M are initialized as the identity matrix. We carefully set other parameters for these methods via cross validation. The results are listed in Table. 1, in which the best ones are bolded. Both our p -BDML and t -BDML perform well on these datasets. Especially, t -BDML is consistently better than p -BDML which validates the effectiveness of triplet constraints as suggested by [39].

We then demonstrate how the performance of the kNN classifier varies according to the condition number of the learned metric in Fig. 2. The x-axis is the natural logarithm of the condition number. It is clear from the figure that, the average test errors of both p -BDML and t -BDML first decrease and then increase when the condition numbers become larger. These results provide strong evidence to support our previous analysis that a largely distorted metric space leads to overfitting and a small distortion may result in underfitting. And our BDML effectively controls the distortion, thus improving the generalization ability.

7.2 Domain Adaptation

We also apply our BDML to domain adaptation problems, under both unsupervised and semi-supervised settings. In the former case, we labeled samples in a source domain for training and want to test the unlabeled samples in the target domain. While in the later setting, apart from labeled samples in a source domain, a small number of labeled samples in the target domain are also accessible during training. We use the same dataset as in [35], which contains 2,533 images of 10 categories from 4 domains: Caltech, Amazon, Webcam, and Dslr. We exploit the same 10 categories as [10] to all the four domains. Experiments are repeated with 20 fixed train/test splits offered by [35]. We set the number of neighbors of kNN to 1 as other methods. Since the original SURF feature is of 800 dimension, we perform pseudometric learning with t -BDML and initialize the dimension-reduction mapping via PCA. The size of mapping matrix is set to 30×800 according to cross-validation.

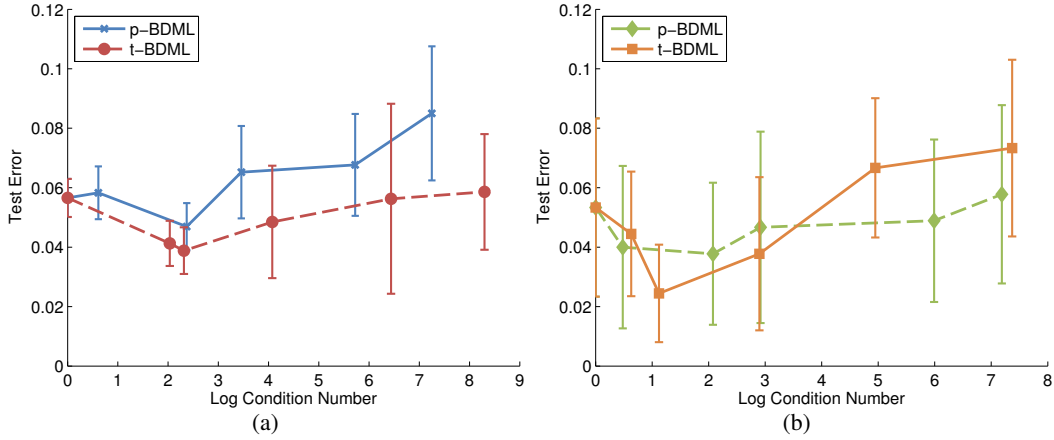


Figure 2: Average test error varies with the natural logarithm of condition number on (a) Segment and (b) Iris datasets.

Methods	A \rightarrow C	A \rightarrow W	C \rightarrow A	C \rightarrow D	D \rightarrow A	D \rightarrow W	W \rightarrow A	W \rightarrow D
OrigFeat	22.6(0.3)	23.5(0.6)	20.8(0.4)	22.0(0.6)	27.7(0.4)	53.1(0.6)	20.7(0.6)	37.3(1.2)
SGF	35.3(0.5)	31.0(0.7)	36.8(0.5)	32.6(0.8)	32.0(0.4)	66.0(0.5)	27.5(0.5)	54.3(1.2)
GFK	35.6(0.4)	34.4(0.9)	36.9(0.4)	35.2(1.0)	32.5(0.5)	74.9(0.6)	31.1(0.8)	70.6(0.9)
LMNN	35.7(0.5)	32.9(0.8)	33.8(0.7)	31.5(1.6)	33.7(0.4)	75.1(0.8)	30.8(0.7)	67.6(1.0)
DML-eig	35.0(0.7)	28.9(0.7)	33.7(0.7)	32.7(1.3)	33.4(0.3)	78.2(0.8)	32.5(0.9)	72.4(0.6)
<i>t</i> -BDML	37.2(0.3)	35.2(1.0)	35.2(0.7)	33.4(1.3)	37.1(0.6)	78.6(0.7)	33.2(0.8)	73.8(0.6)
OrigFeat(semi)	24.0(0.3)	31.6(0.6)	23.1(0.4)	26.5(0.7)	31.3(0.7)	55.5(0.7)	30.8(0.6)	44.3(1.0)
ITML(semi)	27.3(0.7)	36.0(1.0)	33.7(0.8)	35.0(1.1)	30.3(0.8)	55.6(0.7)	32.3(0.8)	51.3(0.9)
SGF(semi)	37.7(0.5)	37.9(0.7)	40.2(0.7)	36.6(0.8)	39.2(0.7)	69.5(0.9)	38.2(0.6)	60.6(1.0)
GFK(semi)	37.8(0.4)	53.7(0.8)	42.0(0.5)	49.5(0.9)	45.0(0.7)	78.7(0.5)	42.8(0.7)	75.0(0.7)
LMNN(semi)	36.6(0.6)	49.6(0.9)	43.3(0.5)	50.3(1.3)	42.0(0.7)	78.6(0.7)	42.3(0.6)	72.8(1.1)
DML-eig (semi)	27.8(0.7)	40.5(1.0)	43.3(0.6)	45.1(1.6)	43.4(0.6)	80.5(0.9)	40.8(0.7)	76.8(0.9)
<i>t</i> -BDML(semi)	38.8(0.3)	55.8(1.1)	44.6(0.6)	54.0(1.1)	43.9(0.6)	83.8(0.5)	44.8(0.6)	79.2(0.7)

Table 2: Comparison of unsupervised (upper part) and semi-supervised (lower part denoted with “semi”) domain adaptation. Mean test accuracy (%) and standard error (inside parentheses) are reported.

Table 2 presents the mean test accuracy and standard errors of various metric learning based methods, including LMNN [39], ITML [35], SGF [11], GFK [10] and DML-eig [42], where A \rightarrow C means the adaptation from source domain A (*i.e.*, Amazon) to the target domain C (*i.e.*, Caltech). And for fair competition, we adopt the best results of GFK under the PCA subspace setting reported by [10]. The results in the original Euclidean space are denoted as OrigFeat. In most subtasks of these two settings, our *t*-BDML outperforms than other competitors which demonstrates the strength of the proposed pseudo-metric learning scheme.

7.3 Face Verification

Finally, we apply our BDML to an unconstrained face verification task, using the large-scale LFW dataset that contains 13,233 face images of 5,749 people. It is challenging due to the large variations of faces in illumination, expression, pose, resolution, etc. There are 6 standard protocols [18] for evaluating results. We use the setting called “Image-Restricted, Label-Free Outside Data”, where we can only access the provided labeled pairs of faces during training. Thus we only compare pseudo-metric learning of *p*-BDML since using triplet constraints would violate this setting. The dataset is organized in 10 folders and each of them contains 300 similar pairs of faces and 300 dissimilar ones. The reported accuracy is obtained via cross validation on the provided 10 folds.

Current state-of-the-art methods under this setting often build various classifiers and combine multiple types of visual descriptors. Since we primarily aim at validating the effectiveness of BDML, we do not carry out intensive feature engineering or build complex similarity measurements. Instead,

Methods	Mean Cond. Num.	Mean Acc.	Std Err.
Xing	—	0.7593	0.0059
ITML	1.2037	0.7812	0.0045
LDML	—	0.7927	0.0060
DML-eig	3228.4	0.8127	0.0230
Sub-ITML	1.2157	0.8145	0.0046
KISSME	—	0.8308	0.0056
Sub-ML	1171.397	0.8330	0.0026
p -BDML	8.3771	0.8632	0.0022

Table 3: Results of face verification on LFW, where “—” means not applicable due to no public implementation or an unbounded condition number.

we use the public “funneled” SIFT feature³ and regard the learned distance metric as the similarity measure. Since the dimension of raw SIFT feature is too large ($\approx 4k$), we reduce it to 800 via PCA before pseudo-metric learning with p -BDML and set the size of dimension-reduction mapping as 300×800 .

In Table 3, we present results of p -BDML and other metric learning based methods including Xing [41], ITML [7], LDML [12], KISSME [25], DML-eig [42], Sub-ITML and Sub-ML [6]. We also report the average condition number. The ITML methods optimize a logDet regularizer, which yield condition numbers close to one. It suggests that the metric space is not sufficiently distorted for good generalization performance. While the F-norm based regularization methods (*e.g.*, Sub-ML) yield too large distortion, which is not good for generalization. These results support our theoretical analysis in Sec. 6 again. In contrast, our BDML method obtains an appropriate condition number, which results in decent generalization performance. Full comparison (including ROC curves) with other non-distance based methods is presented in the appendix.

8 Conclusions

In this paper, we propose the bounded-distortion metric learning (BDML), which well-balances the fitness to data and the distortion of metric embedding. For Mahalanobis metric space, BDML leads to a bounded condition number metric learning method, which possesses intriguing properties. We propose an efficient learning algorithm and further provide theoretical analysis, which explains why the distortion is a key ingredient to ensure good generalization ability. Also, we generalize to pseudo-metric learning and propose an approximate solver based on the semidefinite relaxation and a randomised algorithm. Empirical results validate that our BDML leads to both better generalization and well-conditionness. In future, we would like to extend the distortion to non-Mahalanobis metric and design corresponding approximation algorithms.

³<http://lear.inrialpes.fr/people/guillaumin/data.php>

9 Appendix

9.1 Proofs in Section 3

Proof of Proposition 1.

Proof. Note that for any two different points x, y , we have,

$$\frac{d_M(f(x), f(y))}{d_I(x, y)} = \frac{(x - y)^\top M(x - y)}{(x - y)^\top (x - y)}.$$

It is easy to see that above equation is the Rayleigh quotient of the PSD matrix M . Therefore,

$$\lambda_{\min} \leq \frac{d_M(f(x), f(y))}{d_I(x, y)} \leq \lambda_{\max},$$

where λ_{\min} and λ_{\max} are the minimum and maximum eigenvalue of M respectively. According to the Definition 2, setting $r = \lambda_{\min}$, we can find that for any $c \geq \frac{\lambda_{\max}}{\lambda_{\min}}$, it is always true,

$$r \cdot d_{\mathcal{X}}(x, y) \leq d_{\mathcal{Y}}(f(x), f(y)) \leq cr \cdot d_{\mathcal{X}}(x, y).$$

Hence the distortion of the metric embedding $f_{I \rightarrow M}$ is $\inf\{c | c \geq \frac{\lambda_{\max}}{\lambda_{\min}}\} = \kappa(M)$.

Q.E.D.

9.2 Proofs in Section 4

Proof of Lemma 1.

Proof. If Y^* is a feasible solution of problem (5), then $J_i \bullet Y^* \geq h_i, \forall i$. Since $\forall i, 0 \leq p_i \leq 1$, we have $\sum_{i=1}^m p_i (J_i \bullet Y^* - h_i) \geq 0$. Hence, Y^* is also a feasible solution of problem (6).

If there exists a probability vector \mathbf{p} such that the problem (6) is infeasible, then for all $Y \in \mathbb{P}_R^{3d+1}$, we have $\sum_{i=1}^m p_i (J_i \bullet Y - h_i) < 0$. Therefore, the original problem (5) is also infeasible, since otherwise there exists a solution \tilde{Y} such that $\tilde{Y} \in \mathbb{P}_R^{3d+1}$ and $\sum_{i=1}^m p_i (J_i \bullet \tilde{Y} - h_i) \geq 0$.

Q.E.D.

Proof of Theorem 1.

Proof. In the t -th round, we run the ORACLE with a probability distribution $p^{(t)}$ as input.

If the ORACLE declares the problem (6) is infeasible, then due to Lemma. 1, the original problem is correctly concluded as infeasible.

On the other hand, if this situation never happens during the iteration, i.e., for any round t , ORACLE succeeds to find a solution $Y^{(t)}$ to problem (6), then we can get the following inequality, $\forall t = 1, 2, \dots, T$,

$$\sum_{i=1}^m p_i^{(t)} \eta_i^{(t)} = \frac{1}{\rho} \sum_{i=1}^m p_i^{(t)} (J_i \bullet Y^{(t)} - h_i) \geq 0,$$

Then, equipped with the above inequality and Theorem 2 in [23], we have, for any constraint i ,

$$\begin{aligned}
0 &\leq \sum_{t=1}^T \eta_i^{(t)} + \varepsilon \sum_{t=1}^T |\eta_i^{(t)}| + \frac{\ln(m)}{\varepsilon} \\
&= \frac{1}{\rho} \sum_{t=1}^T (J_i \bullet Y^{(t)} - h_i) \\
&\quad + \frac{\varepsilon}{\rho} \sum_{t=1}^T |J_i \bullet Y^{(t)} - h_i| + \frac{\ln(m)}{\varepsilon} \\
&= \frac{(1+\varepsilon)}{\rho} \sum_{t=1}^T (J_i \bullet Y^{(t)} - h_i) \\
&\quad + \frac{2\varepsilon}{\rho} \sum_{t \in \mathcal{T}_-} |J_i \bullet Y^{(t)} - h_i| + \frac{\ln(m)}{\varepsilon} \\
&\leq \frac{(1+\varepsilon)}{\rho} \sum_{t=1}^T (J_i \bullet Y^{(t)} - h_i) + 2\varepsilon T + \frac{\ln(m)}{\varepsilon}.
\end{aligned}$$

Here \mathcal{T}_- denotes the set of index t when $J_i \bullet Y^{(t)} - h_i < 0$. Divided by T on both sides of the above inequality and with some rearrangement, we can obtain,

$$J_i \bullet \left(\frac{1}{T} \sum_{t=1}^T Y^{(t)} \right) - h_i \geq -\frac{\rho}{1+\varepsilon} \left(2\varepsilon + \frac{\ln(m)}{\varepsilon T} \right).$$

Note that $\bar{Y} = (\sum_{t=1}^T Y^{(t)})/T$ is the solution returned by the multiplicative weights update method. Now, if we set $\varepsilon = \frac{C_1 \delta}{\rho}$, $T = \frac{C_2 \rho^2 \ln(m)}{\delta^2}$, where C_1, C_2 are positive real numbers, then we have,

$$-\frac{\rho}{1+\varepsilon} \left(2\varepsilon + \frac{\ln(m)}{\varepsilon T} \right) = -\frac{\rho}{\rho + C_1 \delta} \left(2C_1 + \frac{1}{C_1 C_2} \right) \delta.$$

With some calculation, we can find that if we choose $0 < C_1 < 1/2$ and set $C_2 = -\frac{1}{C_1(2C_1-1)}$, e.g., $C_1 = 1/4, C_2 = 8$, then $J_i \bullet \bar{Y} - h_i \geq -\delta/(1 + \frac{\delta}{4\rho}) \geq -\delta$ for any constraint i .

Q.E.D.

9.3 Proofs in Section 5

Proof of Proposition 2.

Proof. We first restate problem (7) as below,

$$\begin{aligned}
\min_{Q \in \mathbb{R}^{q \times d}} \quad & \frac{1}{n} \sum_{(i,j) \in \mathcal{S}} X_{ij} \bullet (Q^\top \Lambda Q) \\
s.t. \quad & X_{ij} \bullet (Q^\top \Lambda Q) \geq \mu, \quad \forall (i,j) \in \mathcal{I}, \quad (10a) \\
& Q Q^\top = I. \quad (10b)
\end{aligned}$$

We can denote the vectorization of Q as ζ and rewrite the above problem as the following standard formulation of quadratic constrained quadratic programming (QCQP),

$$\begin{aligned}
\min_{\zeta \in \mathbb{R}^{qd \times 1}} \quad & \frac{1}{n} \sum_{(i,j) \in \mathcal{S}} \zeta^\top \tilde{X}_{ij} \zeta \\
s.t. \quad & \zeta^\top \tilde{X}_{ij} \zeta \geq \mu, \quad \forall (i,j) \in \mathcal{I}, \quad (11a) \\
& \zeta^\top A_{uv} \zeta = b_{uv}, \quad \forall (u,v) \in \mathcal{C}, \quad (11b)
\end{aligned}$$

where the set of margin constraints in (10a) corresponds to the one in (11a) and the set of orthogonal constraints in (10b) corresponds to the one in (11b). Specifically, $\tilde{X}_{ij} = X_{ij} \otimes \Lambda$ and \otimes stands for Kronecker product. And we denote the index set of the upper triangular part of a q -dimensional

squared matrix as $\mathcal{C} = \{(u, v) \in [q] \times [q] | u \leq v\}$ where $[q] = \{1, 2, \dots, q\}$. Then for each element (u, v) of \mathcal{C} , we have A_{uv} is a block diagonal matrix which contains d identical blocks $B_{uv} \in \mathbb{R}^{q \times q}$ as following,

$$A_{uv} = \begin{pmatrix} B_{uv} & & \\ & B_{uv} & \\ & & \ddots \\ & & & B_{uv} \end{pmatrix}$$

where

$$B_{uv} = \begin{pmatrix} & u & v & \\ & & & \\ & & & \\ \dots & \vdots & 1 & \dots \\ \dots & 1 & \vdots & \dots \\ & \vdots & & \end{pmatrix} \begin{matrix} u \\ v \end{matrix}$$

i.e., (u, v) and (v, u) -th entries of B are 1 while others are 0. And $b_{uv} = 2$ if $u = v$, otherwise $b_{uv} = 0$.

Based on [29], to derive the SDP relaxation, we can easily observe the following,

$$\zeta^\top \tilde{X}_{ij} \zeta = \text{Tr}(\tilde{X}_{ij} \zeta \zeta^\top) = \tilde{X}_{ij} \bullet \zeta \zeta^\top.$$

Thus setting $\tilde{Q} = \zeta \zeta^\top$, we can write the equivalent form of the above QCQP as below,

$$\begin{aligned} \min_{\zeta \in \mathbb{R}^{qd \times 1}} \quad & \frac{1}{n} \sum_{(i,j) \in \mathcal{S}} \tilde{X}_{ij} \bullet \tilde{Q} \\ \text{s.t.} \quad & \tilde{X}_{ij} \bullet \tilde{Q} \geq \mu, & \forall (i, j) \in \mathcal{I}, \\ & A_{uv} \bullet \tilde{Q} = b_{uv}, & \forall (u, v) \in \mathcal{C}, \\ & \text{rank}(\tilde{Q}) = 1. \end{aligned}$$

By removing the last rank constraint, we can obtain the desired SDP relaxation.

Q.E.D.

Remark. Note that the orthogonal constraints in the original QCQP problem imply that $\text{Tr}(\tilde{Q}) = q$ in the SDP relaxation problem.

Before obtaining our **Theorem 2**, we need to introduce three lemmas as below. First, we state the Lemma 1 in [30] as below which gives the polynomial tail bound of the left-side inequality $\xi^\top H \xi < \gamma \mathbb{E}[\xi^\top H \xi]$. Reader can refer to the paper for details of the proof.

Lemma 3 (Left-side Polynomial Tail Bound). *Let $H \in \mathbb{S}_+^d, Z \in \mathbb{S}_+^d$. Suppose $\xi \in \mathbb{R}^d$ is a random vector generated from the real-valued normal distribution $\mathcal{N}(0, Z)$. Then for any $\gamma > 0$,*

$$\text{Prob}(\xi^\top H \xi < \gamma \mathbb{E}[\xi^\top H \xi]) < \max\{\sqrt{\gamma}, \frac{2(\bar{r} - 1)\gamma}{\pi - 2}\},$$

where $\bar{r} = \min\{\text{rank}(H), \text{rank}(Z)\}$.

Then we derive a right-side exponential tail bound as below.

Lemma 4 (Right-side Exponential Tail Bound). *Let $H \in \mathbb{S}_+^d, Z \in \mathbb{S}_+^d$. Suppose $\xi \in \mathbb{R}^d$ is a random vector generated from the real-valued normal distribution $\mathcal{N}(0, Z)$. Then for any $\gamma \geq 1$,*

$$\text{Prob}(\xi^\top H \xi > \gamma \mathbb{E}[\xi^\top H \xi]) < \bar{r} \exp\left(-\frac{1}{2}(\gamma - \sqrt{2\gamma - 1})\right),$$

where $\bar{r} = \min\{\text{rank}(H), \text{rank}(Z)\}$.

Proof. Let $r = \text{rank}(Z)$. Since $Z \in \mathbb{S}_+^d$, then we can write $Z = UU^\top$ for some $U \in \mathbb{R}^{d \times r}$. We consider the eigen decomposition of the real symmetric matrix $U^\top HU = LDL^\top = \sum_{i=1}^r \lambda_i l_i l_i^\top$, where $L = [l_1, l_2, \dots, l_r] \in \mathbb{R}^{r \times r}$ is an orthogonal matrix and $D = \text{diag}\{\lambda_1, \lambda_2, \dots, \lambda_r\}$ with $\lambda_1 \geq \lambda_2 \geq \dots \geq \lambda_r \geq 0$. Note that $\lambda_i = 0$ for all $i > \bar{r}$ due to the fact that $U^\top HU$ has rank at most \bar{r} . Denoting $\bar{\xi} \sim \mathcal{N}(0, I_r)$, then we can easily check that $U\bar{\xi} \sim \mathcal{N}(0, Z)$, i.e., $U\bar{\xi}$ is statistically identical to ξ .

Therefore, we have that,

$$\begin{aligned} \text{Prob}(\xi^\top H \xi > \gamma \mathbb{E}[\xi^\top H \xi]) &= \text{Prob}(\bar{\xi}^\top U^\top H U \bar{\xi} > \gamma \mathbb{E}[\bar{\xi}^\top U^\top H U \bar{\xi}]) \\ &= \text{Prob}\left(\sum_{i=1}^{\bar{r}} \lambda_i (l_i^\top \bar{\xi})^2 > \gamma \mathbb{E}\left[\sum_{i=1}^{\bar{r}} \lambda_i (l_i^\top \bar{\xi})^2\right]\right) \end{aligned}$$

Denoting $u_i = l_i^\top \bar{\xi}$, we have that $\mathbb{E}[u_i] = 0$ and $\mathbb{E}[u_i^2] = 1$, i.e., u_i is a standard normal variable. Hence,

$$\begin{aligned} \text{Prob}(\xi^\top H \xi > \gamma \mathbb{E}[\xi^\top H \xi]) &= \text{Prob}\left(\sum_{i=1}^{\bar{r}} \lambda_i u_i^2 > \gamma \mathbb{E}\left[\sum_{i=1}^{\bar{r}} \lambda_i u_i^2\right]\right) \\ &= \text{Prob}\left(\sum_{i=1}^{\bar{r}} \lambda_i u_i^2 > \gamma \sum_{i=1}^{\bar{r}} \lambda_i\right) \\ &= \text{Prob}\left(\sum_{i=1}^{\bar{r}} \bar{\lambda}_i u_i^2 > \gamma\right), \end{aligned}$$

where $\bar{\lambda}_i = \lambda_i / \sum_{i=1}^{\bar{r}} \lambda_i$ for $i = 1, \dots, \bar{r}$. Note that $\sum_{i=1}^{\bar{r}} \bar{\lambda}_i = 1$ and $\bar{\lambda}_1 \geq \bar{\lambda}_2 \geq \dots \geq \bar{\lambda}_{\bar{r}} \geq 0$. Then

$$\begin{aligned} \text{Prob}\left(\sum_{i=1}^{\bar{r}} \bar{\lambda}_i u_i^2 > \gamma\right) &= 1 - \text{Prob}\left(\sum_{i=1}^{\bar{r}} \bar{\lambda}_i u_i^2 \leq \gamma\right) \\ &\leq 1 - \text{Prob}(u_1^2 \leq \gamma \ \& \ \dots \ \& \ u_{\bar{r}}^2 \leq \gamma) \\ &= \text{Prob}(u_1^2 > \gamma \ \parallel \ \dots \ \parallel \ u_{\bar{r}}^2 > \gamma) \\ &\leq \sum_{i=1}^{\bar{r}} \text{Prob}(u_i^2 > \gamma) \\ &\leq \bar{r} \exp\left(-\frac{1}{2}(\gamma - \sqrt{2\gamma - 1})\right) \end{aligned}$$

Note that the last step is due to the inequality in Lemma (7) and the fact that u_i^2 is a χ^2 random variable with 1 degree of freedom.

Q.E.D.

At last, we derive another two-side exponential tail bound for our own purpose.

Lemma 5 (Two-side Exponential Tail Bound). Let $\tilde{Q}^* \in \mathbb{S}_+^{qd}$ be the optimal solution of problem (8), and $A_{uv} \in \mathbb{S}^{qd}$ be any constraint matrix corresponding to index set \mathcal{C} in problem (8). Suppose $\xi \in \mathbb{R}^{qd}$ is a random vector generated from the real-valued normal distribution $\mathcal{N}(0, \tilde{Q}^*)$. Then for any $\epsilon \geq 0$

$$\text{Prob}(|\xi^\top A_{uv} \xi - \mathbb{E}[\xi^\top A_{uv} \xi]| \geq \epsilon) \leq \bar{r} \left[\exp\left(-\frac{(\tau - 1)^2}{4}\right) + \exp\left(-\frac{\epsilon^2}{8\bar{r}dq^2}\right) \right],$$

where $\bar{r} = \min\{\text{rank}(A_{uv}), \text{rank}(\tilde{Q}^*)\}$ and $\tau = \left(\frac{\epsilon}{q} \sqrt{\frac{2}{\bar{r}d}} + 1\right)^{\frac{1}{2}}$.

Proof. Let $r = \text{rank}(\tilde{Q}^*)$. Since $\tilde{Q}^* \in \mathbb{S}_+^{qd}$, we can write $\tilde{Q}^* = UU^\top$ for some $U \in \mathbb{R}^{qd \times r}$. And since A_{uv} is symmetric, we can write the eigen-decomposition of matrix $U^\top A_{uv} U = LDL^\top$,

where $L = [l_1, l_2, \dots, l_r] \in \mathbb{R}^{r \times r}$ is an orthogonal matrix and $D = \text{diag}\{\lambda_1, \lambda_2, \dots, \lambda_r\}$ with $\lambda_1 \geq \lambda_2 \geq \dots \geq \lambda_r \geq 0$. Note that $\lambda_i = 0$ for all $i > \bar{r}$ due to the fact that $U^\top H U$ has rank at most \bar{r} . Denoting $\bar{\xi} \sim \mathcal{N}(0, I_r)$, then we can easily check that $U\bar{\xi} \sim \mathcal{N}(0, Z)$, i.e., $U\bar{\xi}$ is statistically identical to ξ .

Therefore, we have that,

$$\text{Prob}(|\xi^\top A_{uv}\xi - \mathbb{E}[\xi^\top A_{uv}\xi]| \geq \epsilon) = \text{Prob}\left(\left|\sum_{i=1}^{\bar{r}} \lambda_i (l_i^\top \bar{\xi})^2 - \sum_{i=1}^{\bar{r}} \mathbb{E}[\lambda_i (l_i^\top \bar{\xi})^2]\right| \geq \epsilon\right)$$

Denoting $u_i = l_i^\top \bar{\xi}$, we have that $\mathbb{E}[u_i] = 0$ and $\mathbb{E}[u_i^2] = 1$, i.e., u_i is a standard normal variable. Hence,

$$\begin{aligned} \text{Prob}(|\xi^\top A_{uv}\xi - \mathbb{E}[\xi^\top A_{uv}\xi]| \geq \epsilon) &= \text{Prob}\left(\left|\sum_{i=1}^{\bar{r}} \lambda_i (u_i^2 - 1)\right| \geq \epsilon\right) \\ &\leq \text{Prob}\left(\sqrt{\sum_{i=1}^{\bar{r}} \lambda_i^2} \sqrt{\sum_{i=1}^{\bar{r}} (u_i^2 - 1)^2} \geq \epsilon\right) \\ &= \text{Prob}\left(\|D\|_F \sqrt{\sum_{i=1}^{\bar{r}} (u_i^2 - 1)^2} \geq \epsilon\right) \end{aligned}$$

Note that,

$$\|D\|_F = \|U^\top A_{uv} U\|_F \leq \|A_{uv}\|_F \|U\|_F^2 = \|A_{uv}\|_F \text{Tr}(\tilde{Q}^*) \leq q\sqrt{2d}.$$

Here the first equality uses the fact that Frobenius norm is rotation-invariant. The second inequality uses the Cauchy-Schwarz inequality. While for the last equality, we can see that if $u = v$, then $\|A_{uv}\|_F = \sqrt{d}$, otherwise $\|A_{uv}\|_F = \sqrt{2d}$. Moreover, we have $\text{Tr}(\tilde{Q}^*) = q$ due to the fact \tilde{Q}^* is the optimal solution of problem (8) satisfying the orthogonal constraints. Therefore, we have that,

$$\begin{aligned} \text{Prob}(|\xi^\top A_{uv}\xi - \mathbb{E}[\xi^\top A_{uv}\xi]| \geq \epsilon) &\leq \text{Prob}\left(\sum_{i=1}^{\bar{r}} (u_i^2 - 1)^2 \geq \frac{\epsilon^2}{2dq^2}\right) \\ &= 1 - \text{Prob}\left(\sum_{i=1}^{\bar{r}} (u_i^2 - 1)^2 < \frac{\epsilon^2}{2dq^2}\right) \\ &\leq 1 - \text{Prob}\left((u_1^2 - 1)^2 < \frac{\epsilon^2}{2\bar{r}dq^2} \ \& \ \dots \ \& \ (u_{\bar{r}}^2 - 1)^2 < \frac{\epsilon^2}{2\bar{r}dq^2}\right) \\ &= \text{Prob}\left((u_1^2 - 1)^2 \geq \frac{\epsilon^2}{2\bar{r}dq^2} \ \parallel \ \dots \ \parallel \ (u_{\bar{r}}^2 - 1)^2 \geq \frac{\epsilon^2}{2\bar{r}dq^2}\right) \\ &\leq \sum_{i=1}^{\bar{r}} \text{Prob}\left((u_i^2 - 1)^2 \geq \frac{\epsilon^2}{2\bar{r}dq^2}\right) \\ &= \sum_{i=1}^{\bar{r}} \text{Prob}\left(|u_i^2 - 1| \geq \frac{\epsilon}{q\sqrt{2\bar{r}d}}\right) \\ &= \sum_{i=1}^{\bar{r}} \left[\text{Prob}\left(u_i^2 \geq 1 + \frac{\epsilon}{q\sqrt{2\bar{r}d}}\right) + \text{Prob}\left(u_i^2 \leq 1 - \frac{\epsilon}{q\sqrt{2\bar{r}d}}\right) \right] \\ &\leq \bar{r} \left[\exp\left(-\frac{(\tau-1)^2}{4}\right) + \exp\left(-\frac{\epsilon^2}{8\bar{r}dq^2}\right) \right]. \end{aligned}$$

where $\tau = \left(\frac{\epsilon}{q\sqrt{\frac{2}{\bar{r}d}}} + 1\right)^{\frac{1}{2}}$. In the last step, we use the exponential tail bound of Chi-square variable in Lemma 7.

Q.E.D.

Remark. Note that if $u = v$ then $\text{rank}(A_{uv}) = d$ otherwise $\text{rank}(A_{uv}) = 2d$. Thus, we have that $\bar{r} \leq 2d$, which could be used to eliminate the variable \bar{r} in the tail bound.

Proof of Theorem 2.

Proof. First, We have the following,

$$\begin{aligned}
& \text{Prob}\left(\nu \geq \gamma\mu \ \& \ \zeta \leq \epsilon \ \& \ \xi^\top \tilde{G}\xi \leq \omega \mathbb{E}[\xi^\top \tilde{G}\xi]\right) \\
& \geq 1 - \text{Prob}\left(\exists(i, j) \ \xi^\top \tilde{X}_{ij}\xi < \gamma\mu\right) - \text{Prob}\left(\exists(u, v) \ |\xi^\top A_{uv}\xi - b_{uv}| > \epsilon\right) - \text{Prob}\left(\xi^\top \tilde{G}\xi > \omega \mathbb{E}[\xi^\top \tilde{G}\xi]\right) \\
& \geq 1 - \sum_{(i, j) \in \mathcal{I}} \text{Prob}\left(\xi^\top \tilde{X}_{ij}\xi < \gamma\mu\right) - \sum_{(u, v) \in \mathcal{C}} \text{Prob}\left(|\xi^\top A_{uv}\xi - b_{uv}| > \epsilon\right) - \text{Prob}\left(\xi^\top \tilde{G}\xi > \omega \mathbb{E}[\xi^\top \tilde{G}\xi]\right) \\
& = 1 - |\mathcal{I}| + \sum_{(i, j) \in \mathcal{I}} \text{Prob}\left(\xi^\top \tilde{X}_{ij}\xi \geq \gamma\mu\right) - \sum_{(u, v) \in \mathcal{C}} \text{Prob}\left(|\xi^\top A_{uv}\xi - b_{uv}| > \epsilon\right) - \text{Prob}\left(\xi^\top \tilde{G}\xi > \omega \mathbb{E}[\xi^\top \tilde{G}\xi]\right).
\end{aligned}$$

Here we use the fact that ,

$$\begin{aligned}
\mathbb{E}[\xi^\top \tilde{X}_{ij}\xi] &= \tilde{X}_{ij} \bullet \tilde{Q}^* \geq \mu \\
\mathbb{E}[\xi^\top A_{uv}\xi] &= A_{uv} \bullet \tilde{Q}^* = b_{uv}.
\end{aligned}$$

We denote

$$\begin{aligned}
\mathbb{T}_1 &= \sum_{(i, j) \in \mathcal{I}} \text{Prob}\left(\xi^\top \tilde{X}_{ij}\xi \geq \gamma\mu\right), \\
\mathbb{T}_2 &= \sum_{(u, v) \in \mathcal{C}} \text{Prob}\left(|\xi^\top A_{uv}\xi - b_{uv}| > \epsilon\right) \\
\mathbb{T}_3 &= \text{Prob}\left(\xi^\top \tilde{G}\xi > \omega \mathbb{E}[\xi^\top \tilde{G}\xi]\right).
\end{aligned}$$

and

$$\begin{aligned}
r_1 &= \min\{\max_{(i, j)} \text{rank}(\tilde{X}_{ij}), \text{rank}(\tilde{Q}^*)\}, \\
r_2 &= \min\{\max_{(u, v)} \text{rank}(A_{uv}), \text{rank}(\tilde{Q}^*)\}, \\
r_3 &= \min\{\text{rank}(\tilde{G}), \text{rank}(\tilde{Q}^*)\}.
\end{aligned}$$

According to the first constraints in (8) and the lemma of left-side polynomial tail bound, we have,

$$\begin{aligned}
\mathbb{T}_1 &\geq \sum_{(i, j) \in \mathcal{I}} \text{Prob}\left(\xi^\top \tilde{X}_{ij}\xi \geq \gamma \mathbb{E}[\xi^\top \tilde{X}_{ij}\xi]\right) \\
&\geq |\mathcal{I}| \left(1 - \max\{\sqrt{\gamma}, \frac{2(r_1 - 1)\gamma}{\pi - 2}\}\right).
\end{aligned}$$

Then according the second constraints in (8) and the lemma of two-side exponential tail, we have,

$$\begin{aligned}
\mathbb{T}_2 &= \sum_{(u, v) \in \mathcal{C}} \text{Prob}\left(|\xi^\top A_{uv}\xi - \mathbb{E}[\xi^\top A_{uv}\xi]| > \epsilon\right) \\
&\leq \frac{r_2 q(q+1)}{2} \left[\exp\left(-\frac{(\tau - 1)^2}{4}\right) + \exp\left(-\frac{\epsilon^2}{8r_2 dq^2}\right) \right],
\end{aligned}$$

where $\tau = \left(\frac{\epsilon}{q} \sqrt{\frac{2}{r_2 d}} + 1\right)^{\frac{1}{2}}$. At last, according to the lemma of right-side exponential tail bound, we have,

$$\mathbb{T}_3 \leq r_3 \exp\left(-\frac{1}{2}(\omega - \sqrt{2\omega - 1})\right).$$

Therefore, based on all above inequalities and facts that $r_1 \leq r$, $r_2 \leq r$ and $r_3 \leq r$, we can derive that,

$$\begin{aligned} \text{Prob} \left(\nu \geq \gamma\mu \quad \& \quad \zeta \leq \epsilon \quad \& \quad \xi^\top \tilde{G} \xi \leq \omega \tilde{G} \bullet \tilde{Q}^* \right) \geq 1 - |\mathcal{I}| \max \left(\sqrt{\gamma}, \frac{2(r-1)\gamma}{\pi-2} \right) \\ - r \exp \left(-\frac{1}{2} (\omega - \sqrt{2\omega-1}) \right) - \frac{rq(q+1)}{2} \left[\exp \left(-\frac{(\tau-1)^2}{4} \right) + \exp \left(-\frac{\epsilon^2}{8rdq^2} \right) \right]. \end{aligned}$$

Q.E.D.

9.4 Proofs in Section 6

Proof of Lemma 2.

Proof. The given loss function is $\ell(\mathcal{A}, X_{ij}) = M \bullet X_{ij}$. First, note that,

$$\begin{aligned} M \bullet X_{ij} &= (x_i - x_j)^\top M (x_i - x_j), \\ &= \frac{(x_i - x_j)^\top M (x_i - x_j)}{(x_i - x_j)^\top (x_i - x_j)} (x_i - x_j)^\top (x_i - x_j), \end{aligned}$$

Then, relying on the property of the Rayleigh quotient, we can obtain that,

$$\lambda_{\min} \|x_i - x_j\|_2^2 \leq M \bullet X_{ij} \leq \lambda_{\max} \|x_i - x_j\|_2^2,$$

where λ_{\max} and λ_{\min} are the maximum and minimum eigenvalues of M .

Thus, denoting the replace-one dataset and the corresponding metric as D^k and M^k respectively, we can derive that,

$$\begin{aligned} |\ell(\mathcal{A}_D, X_{ij}) - \ell(\mathcal{A}_{D^k}, X_{ij})| &= |M \bullet X_{ij} - M^k \bullet X_{ij}|, \\ &\leq |\lambda_{\max} - \lambda_{\min}^k| \|x_i - x_j\|_2^2, \\ &\leq 4\Gamma^2 (\lambda_{\max} + \lambda_{\min}^k), \\ &\leq 4\Gamma^2 \left(\frac{KR}{d} + \frac{R}{d} \right), \\ &\leq \frac{4(K+1)R\Gamma^2}{d}, \end{aligned}$$

where λ_{\max} and λ_{\min}^k are the maximum and minimum eigenvalues of M and M^k respectively. The second inequality uses the fact that x_i and x_j are in a Γ -ball. And the next one relies on that, for both M and M^k , it is true that

$$\lambda_{\max} \leq K\lambda_{\min} \leq \frac{K}{d} \text{Tr}(M) \leq \frac{KR}{d}.$$

Therefore, the Uniform-Replace-One stability $\beta = \frac{4(K+1)R\Gamma^2}{d}$.

Q.E.D.

Remark. Note if our previous assumption is violated, i.e., M is rank-deficient, then this stability result does not stand any more. In particular, we will have, for any M ,

$$\lambda_{\max} \leq K\lambda_{\min} \leq \frac{K}{r} \text{Tr}(M) \leq \frac{KR}{r},$$

where r is the rank of M and $r < d$. Then, the stability could be rewritten as $\beta = \frac{4(K+1)R\Gamma^2}{\bar{r}}$, where $\bar{r} = \min\{\text{rank}(M), \text{rank}(M^k)\}$. This resultant stability is case-dependent, thus being less favourable. This argument is important for our later explanation why our generalization bound will not become tighter and tighter via trivially increasing the feature dimension.

To prove the Theorem 3, we first state one part of **Lemma 9** in [5] as below.

Lemma 6 (Variance Bound). For any algorithm \mathcal{A} and loss function ℓ such that $0 \leq \ell \leq L$, we have for any different $i, j \in \{1, \dots, n\}$,

$$\mathbb{E}_D \left[(\mathcal{R}(\mathcal{A}, D) - \mathcal{R}_{emp}(\mathcal{A}, D))^2 \right] \leq \frac{L^2}{2n} + 3L \mathbb{E}_{\{D \cup z'_i\}} [|\ell(A_D, z_i) - \ell(A_{D^i}, z_i)|].$$

Remark. Here D and D^i are defined in Sect. 6 and $D^i = \{D \setminus z_i \cup z'_i\}$.

Proof of Theorem 3.

Proof. First, for the given loss function ℓ , we have that,

$$\begin{aligned} \ell(\mathcal{A}, X_{ij}) &= M \bullet X_{ij} \\ &\leq \lambda_{\max} \|x_i - x_j\|_2^2 \\ &\leq \frac{4KR\Gamma^2}{d}. \end{aligned}$$

Then due to the definition of uniform-RO stability, we have that

$$\mathbb{E}_{\{D \cup z'_i\}} [|\ell(A_D, z_i) - \ell(A_{D^i}, z_i)|] \leq \beta.$$

Therefore, according to the above lemma of variance bound, we can obtain that,

$$\begin{aligned} \mathbb{E}_D \left[(\mathcal{R}(\mathcal{A}, D) - \mathcal{R}_{emp}(\mathcal{A}, D))^2 \right] \\ \leq \frac{8K^2 R^2 \Gamma^4}{nd^2} + \frac{12KR\Gamma^2 \beta}{d}. \end{aligned}$$

Then based on Chebyshev's inequality, we can derive that,

$$\begin{aligned} \text{Prob}(\mathcal{R}(\mathcal{A}, D) - \mathcal{R}_{emp}(\mathcal{A}, D) \geq \epsilon) \\ \leq \frac{\mathbb{E}_D \left[(\mathcal{R}(\mathcal{A}, D) - \mathcal{R}_{emp}(\mathcal{A}, D))^2 \right]}{\epsilon^2} \\ \leq \frac{1}{\epsilon^2} \left(\frac{8K^2 R^2 \Gamma^4}{nd^2} + \frac{12KR\Gamma^2 \beta}{d} \right). \end{aligned}$$

Setting the right hand side of the above inequality as δ , we thus have with probability at least $1 - \delta$ that,

$$\mathcal{R}(\mathcal{A}, D) \leq \mathcal{R}_{emp}(\mathcal{A}, D) + 2\Gamma \sqrt{\frac{KR}{d\delta} \left(\frac{2KR\Gamma^2}{nd} + 3\beta \right)}.$$

By substituting the Uniform-Replace-One stability β , we can obtain the following specific bound,

$$\mathcal{R}(\mathcal{A}, D) \leq \mathcal{R}_{emp}(\mathcal{A}, D) + \frac{2R\Gamma^2}{d} \sqrt{\frac{2K}{\delta} \left(\frac{K}{n} + 6K + 6 \right)}.$$

Q.E.D.

Remark. As aforementioned, there is one counter-intuitive property of our generalization bound that it becomes tighter when the feature dimension d increases. However, it is the case only if our previous full-rank assumption on M holds. If this assumption is violated, *e.g.*, in the sparse high dimensional feature space, the above result does not stand any more. Therefore, it rules out the possibility that trivially increasing the feature dimension by adding zeros will improve the generalization ability.

K	Mean Cond. Num.	Mean Err.	Std Err.(\pm)
1.0e+1	1.454	4.222	2.446
1.0e+2	2.165	3.333	2.160
1.0e+3	2.158	4.222	2.147
1.0e+4	37.567	5.333	2.859
1.0e+5	2962.094	6.222	3.443

Table 4: Performance varies with distortion bound K .

R	ρ	Mean Cond. Num.	Mean Err.	Std Err.(\pm)
1.0e+2	1.0e+2	2.682	4.222	2.210
1.0e+2	5.0e+2	1.638	4.222	1.640
1.0e+2	1.0e+3	2.354	5.111	1.500
1.0e+3	1.0e+3	2.768	5.778	2.608
1.0e+3	5.0e+3	1.611	4.889	1.753
1.0e+3	1.0e+4	2.360	7.111	2.295

Table 5: Performance varies with trace bound R and width ρ .

10 Impact of Parameters

In this section, we study how the performance of our BDML algorithm varies with several important parameters, including distortion bound K , trace bound R and width ρ . Except running time which needs large scale data, we experiment with all other parameters on the UCI Iris dataset. As in Sect. 7.1, we randomly split the dataset into 70% for training and 30% for testing and report the average test error and its standard deviation by repeating the random splits for 10 times.

10.1 Distortion Bound K

We first study the effects of distortion bound K . We fix the number of iteration $T = 1000$, the margin of p -BDML $\mu = 1$, the trace bound $R = 100$ and the width $\rho = 500$. And we report the mean condition number, mean test error and the standard deviation of test error. The results are listed in Table 10.1. From the table, we can find that with K increases, the resultant mean condition number becomes larger. It is partly because that as K increases, the bounded-distortion constraint becomes easier to satisfy, thus encouraging MWU method puts more weights on other constraints like the margin ones. Hence the learned metric embedding is more distorted to fitting the training data. Moreover, with K increases, the test error first decreases and then increases which matches our analysis in Sect. 6.

10.2 Trace Bound R and Width ρ

We now study the effects of trace bound R and width ρ . These two parameters are correlated in a sense that the width ρ should not be much smaller than the trace bound R since otherwise the constraint of width, i.e., $\forall i, |J_i \bullet Y^{(t)} - h_i| \leq \rho$ will not stand. We fix the number of iteration $T = 1000$, the margin of p -BDML $\mu = 1$ and the distortion bound $K = 1000$. Same measurements are reported in Table 10.2.

From this Table, we can see that if width ρ is set to be much larger than the trace bound R , the resultant mean test error tends to become larger. This may due to the fact that with the same number of iteration, the larger the width, the smaller the overall quality of the solution of the MWU method deteriorates which is matched to the analysis in [23]. On the other side, if width ρ is nearly equal to the trace bound R , the aforementioned constraint of width will be violated sometimes. Therefore, in practice, we find that setting $R \approx 10d$ and $\rho \approx 5R$ yield good results. Here d is the dimension of the input feature.

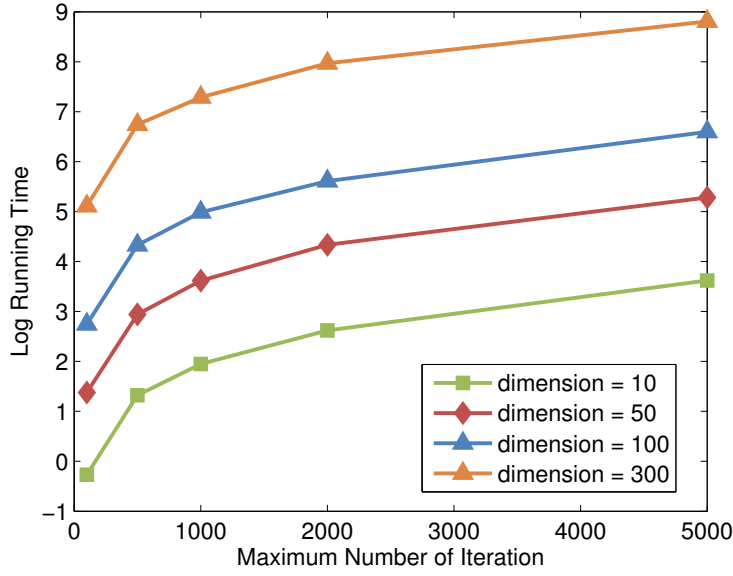


Figure 3: Runing Time of MWU solver.

Methods	OrigFeat	SGF	GFK(PCA)	LMNN	DML-eig	t -BDML
A \rightarrow C	22.6(0.3)	35.3(0.5)	35.6(0.4)	35.7(0.5)	35.0(0.7)	37.2(0.3)
A \rightarrow D	22.2(0.4)	30.7(0.8)	35.2(0.9)	32.3(1.0)	27.6(1.1)	33.0(1.0)
A \rightarrow W	23.5(0.6)	31.0(0.7)	34.4(0.9)	32.9(0.8)	28.9(0.7)	35.2(1.0)
C \rightarrow A	20.8(0.4)	36.8(0.5)	36.9(0.4)	33.8(0.7)	33.7(0.7)	35.2(0.7)
C \rightarrow D	22.0(0.6)	32.6(0.8)	35.2(1.0)	31.5(1.6)	32.7(1.3)	33.4(1.3)
C \rightarrow W	19.4(0.7)	30.6(0.8)	33.7(1.1)	26.0(1.2)	29.2(1.3)	29.6(0.8)
D \rightarrow A	27.7(0.4)	32.0(0.4)	32.5(0.5)	33.7(0.4)	33.4(0.3)	37.1(0.6)
D \rightarrow C	24.8(0.4)	29.4(0.5)	29.8(0.3)	29.4(0.5)	29.8(0.3)	32.6(0.6)
D \rightarrow W	53.1(0.6)	66.0(0.5)	74.9(0.6)	75.1(0.8)	78.2(0.8)	78.6(0.7)
W \rightarrow A	20.7(0.6)	27.5(0.5)	31.1(0.8)	30.8(0.7)	32.5(0.9)	33.2(0.8)
W \rightarrow C	16.1(0.4)	21.7(0.4)	27.2(0.5)	26.3(0.7)	27.0(0.5)	28.5(0.6)
W \rightarrow D	37.3(1.2)	54.3(1.2)	70.6(0.9)	67.6(1.0)	72.4(0.6)	73.8(0.6)

Table 6: Comparison of unsupervised domain adaptation. Mean accuracy (%) and standard error (inside parentheses) are reported. The best performance is denoted in bold type.

10.3 Running Time

We now investigate the running time on the LFW dataset due to its high-dimensional feature. Since the main component of our BDML algorithm is the MWU method, we thus study how its running time varies with respect to the maximum number of iteration and dimension of input feature. The trace bound R and width ρ are both fixed as $3d + 1$ as aforementioned. We implement the algorithm as a single-thread MATLAB program. And all our experiments are conducted on a server with Intel Xeon E5 CPU(2.6GHz) and 128G RAM. In particular, we test following values of dimension d of input feature, 10, 50, 100 and 300. And for each dimension, we set the maximum number of iteration as 100, 500, 1000, 2000 and 5000 and keep track of the corresponding running time. The natural logarithmic of all results are plotted in Fig. 3. Generally, for 100-dim feature, it takes around 146s to finish 1000 iterations of MWU.

11 Full Results of Experiments

We in this section demonstrate the comprehensive results of our experiments.

Methods	OrigFeat	ITML	SGF	GFK(PCA)	LMNN	DML-eig	MMDT	t -BDML
A \rightarrow C	24.0(0.3)	27.3(0.7)	37.7(0.5)	37.8(0.4)	36.6(0.6)	27.8(0.7)	36.4(0.8)	38.8(0.3)
A \rightarrow D	28.1(0.6)	33.7(0.9)	34.5(1.1)	47.0(1.2)	43.8(1.2)	33.0(0.9)	56.7(1.3)	46.5(0.9)
A \rightarrow W	31.6(0.6)	36.0(1.0)	37.9(0.7)	53.7(0.8)	49.6(0.9)	40.5(1.0)	64.6(1.2)	55.8(1.1)
C \rightarrow A	23.1(0.4)	33.7(0.8)	40.2(0.7)	42.0(0.5)	43.3(0.5)	43.3(0.6)	49.4(0.8)	44.6(0.6)
C \rightarrow D	26.5(0.7)	35.0(1.1)	36.6(0.8)	49.5(0.9)	50.3(1.3)	45.1(1.6)	56.5(0.9)	54.0(1.1)
C \rightarrow W	25.2(0.8)	34.7(1.0)	37.2(0.9)	54.2(0.9)	56.2(1.5)	58.9(1.2)	63.8(1.1)	56.0(1.0)
D \rightarrow A	31.3(0.7)	30.3(0.8)	39.2(0.7)	45.0(0.7)	42.0(0.7)	43.4(0.6)	46.9(1.0)	43.9(0.6)
D \rightarrow C	22.4(0.5)	22.5(0.6)	30.2(0.7)	32.7(0.4)	33.4(0.4)	31.9(0.4)	34.1(0.8)	35.4(0.3)
D \rightarrow W	55.5(0.7)	55.6(0.7)	69.5(0.9)	78.7(0.5)	78.6(0.7)	80.5(0.9)	74.1(0.8)	83.8(0.5)
W \rightarrow A	30.8(0.6)	32.3(0.8)	38.2(0.6)	42.8(0.7)	42.3(0.6)	40.8(0.7)	47.7(0.9)	44.8(0.6)
W \rightarrow C	20.8(0.5)	21.7(0.5)	29.2(0.7)	32.8(0.7)	32.2(0.7)	32.8(0.6)	32.2(0.8)	33.3(0.6)
W \rightarrow D	44.3(1.0)	51.3(0.9)	60.6(1.0)	75.0(0.7)	72.8(1.1)	76.8(0.9)	67.0(1.1)	79.2(0.7)

Table 7: Comparison of semi-supervised domain adaptation. Mean accuracy (%) and standard error (inside parentheses) are reported. The best performance is denoted in bold type.

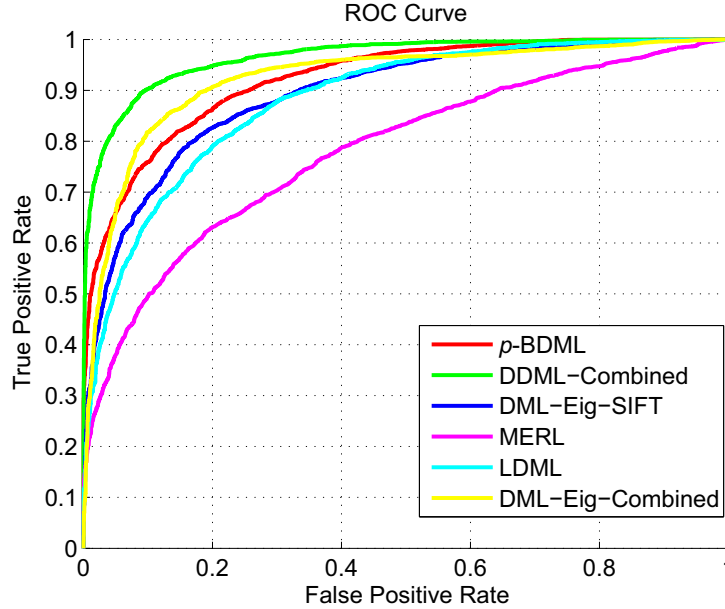


Figure 4: ROC curves on LFW dataset.

11.1 Domain Adaptation

For domain adaptation, we show the full results of all 12 possible combinations of source and target domains. In particular, unsupervised and semi-supervised experiments are listed in Table 6 and Table 7 respectively. We include the state-of-art results of max-margin domain transformations (MMDT) [15] on this dataset in Table 7. Note that the comparison with MMDT is somewhat unfair for our method, because it exploits the discrimination power of a max-margin classifier, whereas ours is the simple distance metric learning based 1-NN classifier. However, it is promising that, with such simple classifier, our BDML still achieves state-of-the-art results in some subtasks.

11.2 Face Verification

In this section, we present full experimental comparisons on LFW dataset. In Table 8, we list various published results on “Image-Restricted, Label-Free Outside Data” setting of LFW dataset. Specifically, the abbreviations of these algorithms are MERL [16], Xing [41], ITML [7], LDML [12], DML-eig-SIFT [42], Sub-ITML [6], KISSME [25], Sub-ML [6], LBP+CSML [31], DML-eig-

Methods	Mean Acc.	Std Err.(±)
MERL	0.7052	0.0060
Xing	0.7593	0.0059
ITML	0.7812	0.0045
LDML	0.7927	0.0060
DML-eig-SIFT	0.8127	0.0230
Sub-ITML	0.8145	0.0046
KISSME	0.8308	0.0056
Sub-ML	0.8330	0.0026
LBP+CSML	0.8557	0.0052
DML-eig-Combined	0.8565	0.0056
p -BDML	0.8632	0.0022
Convolutional DBN	0.8777	0.0062
Sub-SML	0.8973	0.0038
DDML-Combined	0.9068	0.0141

Table 8: Full comparison on “Image-Restricted, Label-Free Outside Data” setting of LFW dataset.

Combined [42], Convolutional DBN [17], Sub-SML [6] and DDML-Combined [22]. Among them, “Convolutional DBN” and “DDML-Combined” are deep learning based methods. Suffix “Combined” means the method uses multiple descriptors, e.g., SIFT [28], LBP [33], TPLBP [40], etc. From this table, we can find that, although using only dimension-reduced SIFT feature, our BDML algorithm achieves comparable results with other feature-combined and non-metric learning based ones. Moreover, our method achieves the least stand errors compared to others which indicates that our BDML produces stable metrics. The ROC curves versus others are plotted in Fig. 4.

12 Useful Tail Bound for Chi-square Variables

We list the following sharp tail bound for chi-square variables.

Lemma 7. [27] Let $X \sim \chi_d^2$ and $\epsilon \geq 0$, then

$$P(X - d \geq 2\sqrt{d\epsilon} + 2\epsilon) \leq \exp(-\epsilon)$$

$$P(X - d \leq -2\sqrt{d\epsilon}) \leq \exp(-\epsilon).$$

References

- [1] S. Arora, E. Hazan, and S. Kale. The multiplicative weights update method: a meta-algorithm and applications. *Theory of Computing*, 8(1):121–164, 2012.
- [2] K. Bache and M. Lichman. UCI machine learning repository, 2013.
- [3] A. Bar-Hillel, T. Hertz, N. Shental, D. Weinshall, and G. Ridgeway. Learning a mahalanobis metric from equivalence constraints. *The Journal of Machine Learning Research*, 6(6), 2005.
- [4] J. Bourgain. On lipschitz embedding of finite metric spaces in hilbert space. *Israel Journal of Mathematics*, 52(1-2):46–52, 1985.
- [5] O. Bousquet and A. Elisseeff. Stability and generalization. *The Journal of Machine Learning Research*, 2:499–526, 2002.
- [6] Q. Cao, Y. Ying, and P. Li. Similarity metric learning for face recognition. In *International Conference on Computer Vision*, 2013.
- [7] J. V. Davis, B. Kulis, P. Jain, S. Sra, and I. S. Dhillon. Information-theoretic metric learning. In *International Conference on Machine Learning*, pages 209–216, 2007.
- [8] M. Der and L. K. Saul. Latent coincidence analysis: A hidden variable model for distance metric learning. In *Advances in Neural Information Processing Systems*, pages 3230–3238, 2012.
- [9] A. Globerson and S. Roweis. Metric learning by collapsing classes. In *Advances in Neural Information Processing Systems*, volume 18, pages 451–458, 2005.

- [10] B. Gong, Y. Shi, F. Sha, and K. Grauman. Geodesic flow kernel for unsupervised domain adaptation. In *Computer Vision and Pattern Recognition*, pages 2066–2073, 2012.
- [11] R. Gopalan, R. Li, and R. Chellappa. Domain adaptation for object recognition: An unsupervised approach. In *International Conference on Computer Vision*, pages 999–1006, 2011.
- [12] M. Guillaumin, J. Verbeek, and C. Schmid. Is that you? metric learning approaches for face identification. In *International Conference on Computer Vision*, pages 498–505, 2009.
- [13] T. Hastie and R. Tibshirani. Discriminant adaptive nearest neighbor classification. *IEEE Transactions on Pattern Analysis and Machine Intelligence*, 18(6):607–616, 1996.
- [14] S. Hauberg, O. Freifeld, and M. J. Black. A geometric take on metric learning. In *Advances in Neural Information Processing Systems*, pages 2033–2041, 2012.
- [15] J. Hoffman, E. Rodner, J. Donahue, T. Darrell, and K. Saenko. Efficient learning of domain-invariant image representations. In *International Conference on Learning Representations*, 2013.
- [16] G. B. Huang, M. J. Jones, E. Learned-Miller, et al. Lfw results using a combined nowak plus merl recognizer. In *Faces in Real-Life Images Workshop in European Conference on Computer Vision (ECCV)*, 2008.
- [17] G. B. Huang, H. Lee, and E. Learned-Miller. Learning hierarchical representations for face verification with convolutional deep belief networks. In *Computer Vision and Pattern Recognition*, pages 2518–2525, 2012.
- [18] G. B. Huang, M. Ramesh, T. Berg, and E. Learned-Miller. Labeled faces in the wild: A database for studying face recognition in unconstrained environments. Technical Report 07-49, University of Massachusetts, Amherst, October 2007.
- [19] P. Indyk and J. Matousek. Low-distortion embeddings of finite metric spaces. *Handbook of Discrete and Computational Geometry*, 37:46, 2004.
- [20] G. Jacob, R. Sam, H. Geoff, and S. Ruslan. Neighbourhood components analysis. In *Advances in Neural Information Processing Systems*, 2004.
- [21] R. Jin, S. Wang, and Y. Zhou. Regularized distance metric learning: theory and algorithm. In *Advances in Neural Information Processing Systems*, volume 22, pages 862–870, 2009.
- [22] Y.-P. T. Junlin Hu, Jiwen Lu. Discriminative deep metric learning for face verification in the wild. In *Computer Vision and Pattern Recognition*, 2014.
- [23] S. Kale. Efficient algorithms using the multiplicative weights update method. *PhD Thesis*, 2007.
- [24] D. Kedem, S. Tyree, K. Q. Weinberger, F. Sha, and G. R. Lanckriet. Non-linear metric learning. In *Advances in Neural Information Processing Systems*, pages 2582–2590, 2012.
- [25] M. Kostinger, M. Hirzer, P. Wohlhart, P. M. Roth, and H. Bischof. Large scale metric learning from equivalence constraints. In *Computer Vision and Pattern Recognition*, pages 2288–2295, 2012.
- [26] G. R. Lanckriet, N. Cristianini, P. Bartlett, L. E. Ghaoui, and M. I. Jordan. Learning the kernel matrix with semidefinite programming. *The Journal of Machine Learning Research*, 5:27–72, 2004.
- [27] B. Laurent and P. Massart. Adaptive estimation of a quadratic functional by model selection. *Annals of Statistics*, pages 1302–1338, 2000.
- [28] D. G. Lowe. Distinctive image features from scale-invariant keypoints. *International Journal of Computer Vision*, 60(2):91–110, 2004.
- [29] Z.-q. Luo, W.-k. Ma, A.-C. So, Y. Ye, and S. Zhang. Semidefinite relaxation of quadratic optimization problems. *IEEE Signal Processing Magazine*, 27(3):20–34, 2010.
- [30] Z.-Q. Luo, N. D. Sidiropoulos, P. Tseng, and S. Zhang. Approximation bounds for quadratic optimization with homogeneous quadratic constraints. *SIAM Journal on Optimization*, 18(1):1–28, 2007.
- [31] H. V. Nguyen and L. Bai. Cosine similarity metric learning for face verification. In *Asian Conference of Computer Vision*, pages 709–720, 2011.
- [32] M. Norouzi, D. J. Fleet, and R. Salakhutdinov. Hamming distance metric learning. In *Advances in Neural Information Processing Systems*, pages 1070–1078, 2012.
- [33] T. Ojala, M. Pietikainen, and T. Maenpaa. Multiresolution gray-scale and rotation invariant texture classification with local binary patterns. *IEEE Transactions on Pattern Analysis and Machine Intelligence*, 24(7):971–987, 2002.

- [34] S. T. Roweis and L. K. Saul. Nonlinear dimensionality reduction by locally linear embedding. *Science*, 290(5500):2323–2326, 2000.
- [35] K. Saenko, B. Kulis, M. Fritz, and T. Darrell. Adapting visual category models to new domains. In *European Conference on Computer Vision*, pages 213–226, 2010.
- [36] S. Shalev-Shwartz, O. Shamir, N. Srebro, and K. Sridharan. Learnability, stability and uniform convergence. *The Journal of Machine Learning Research*, 11:2635–2670, 2010.
- [37] S. Shalev-Shwartz, Y. Singer, and A. Y. Ng. Online and batch learning of pseudo-metrics. In *International Conference on Machine Learning*, page 94, 2004.
- [38] C. Shen, J. Kim, L. Wang, and A. Van Den Hengel. Positive semidefinite metric learning with boosting. In *Advances in Neural Information Processing Systems*, volume 22, pages 629–633, 2009.
- [39] K. Q. Weinberger and L. K. Saul. Distance metric learning for large margin nearest neighbor classification. *The Journal of Machine Learning Research*, 10:207–244, 2009.
- [40] L. Wolf, T. Hassner, Y. Taigman, et al. Descriptor based methods in the wild. In *Workshop on Faces in 'Real-Life' Images: Detection, Alignment, and Recognition*, 2008.
- [41] E. P. Xing, A. Y. Ng, M. I. Jordan, and S. Russell. Distance metric learning with application to clustering with side-information. In *Advances in Neural Information Processing Systems*, pages 521–528, 2003.
- [42] Y. Ying and P. Li. Distance metric learning with eigenvalue optimization. *The Journal of Machine Learning Research*, 13:1–26, 2012.